Heliyon 5 (2019) e01690

Contents lists available at ScienceDirect

Heliyon

www.elsevier.com/locate/heliyon

# Electrode material studies and cell voltage characteristics of the in situ water electrolysis performed in a pH-neutral electrolyte in bioelectrochemical systems

Georgy Givirovskiy [a,*], Vesa Ruuskanen [a], Leo S. Ojala [b], Michael Lienemann [b], Petteri Kokkonen [b], Jero Ahola [a]

[a] LUT University, P.O. Box 20, FI-53851, Lappeenranta, Finland
[b] VTT Technical Research Centre of Finland Ltd., P.O. Box 1000, 02044 VTT, Finland

ARTICLE INFO

*Keywords:*
Bioengineering
Electrochemistry
Materials chemistry

ABSTRACT

Hydrogen-oxidizing bacteria (HOB) have been shown to be promising micro-organisms for the reduction of carbon dioxide to a wide range of value-added products in bioelectrochemical systems with in situ water electrolysis of the cultivation medium, also known as a hybrid biological-inorganic systems (HBI). However, scaling up of this process requires overcoming the inherent constraints of the low energy efficiency partly associated with the pH-neutral electrolyte with low conductivity. Most of the research in the field is concentrated on the bacterial cultivation, whereas the analysis and evaluation of the electrode material performance have received little attention in the literature so far. Therefore, in the present work, in situ electrolysis of a pH-neutral medium for HOB cultivation was performed with different combinations of electrode materials. Besides conventional electrode types, electrodes with coatings made of earth-abundant cobalt and a nickel-iron alloy, known for their catalytic activity for the kinetically sluggish oxygen evolution reaction (OER), were prepared and tested as potential substitutes for catalysts made of precious metals. The cultivation of HOB with in situ water electrolysis has been successfully tested in a small scale electrobioreactor in order to support the experimental results. A simplified water electrolysis model was developed and applied to evaluate the current-voltage characteristics of an bioelectrochemical system prototype. Application of the developed model allows quantitative evaluation and comparison of reversible, ohmic, and activation overvoltages of different electrode sets. The modeling results were found to agree well with the experimental data. The developed model and the data gathered can be applied to further investigation, simulation, and optimization of HBI systems.

## 1. Introduction

The rapid economic growth and the increasing consumption of fossil-fuel-based energy have led to higher concentrations of pollutant gases in the atmosphere, depletion of natural resources, adverse climate impacts, and geopolitical tensions. The global shift from a fossil-fuel-based economy to a renewable-energy-based one has the potential to tackle the aforementioned problems [1, 2]. Electrical energy produced from abundant renewable energy sources, such as solar and wind power, is considered to be the cleanest form of energy. However, the fluctuating nature of these sources leads to technical challenges associated with the storage of the generated electricity [3]. Recently, hydrogen, which is the simplest and lightest element, has been shown to be a sustainable and promising energy carrier in the Hydrogen Economy Concept [4]. Even though the currently dominating technologies of hydrogen production are steam reforming, partial oxidation of hydrocarbons, and coal gasification, the development of advanced technologies for renewable-energy-based hydrogen production is given a high priority, and the topic is attracting scientific interest. One of the most mature technologies of renewable hydrogen production is electrolysis of water [5]. By this method, surplus peak electricity from renewable energy sources is applied to generate renewable hydrogen, which can be further used in Power-to-X processes to produce net carbon-neutral fuels and chemicals [6, 7].

One approach attracting scientific interest in this context is microbial electrosynthesis (MES), electricity-driven synthesis of chemicals

* Corresponding author.
*E-mail address:* georgy.givirovskiy@lut.fi (G. Givirovskiy).

https://doi.org/10.1016/j.heliyon.2019.e01690
Received 19 October 2018; Received in revised form 5 April 2019; Accepted 7 May 2019

and fuels. Microbial electrosynthesis (MES) is an emerging technology capable of using water electrolysis and various microorganisms directly for the reduction of carbon dioxide to value-added compounds in bioelectrochemical systems (BESs). The concept was first proven by Nevin et al. [8], who were able to reduce carbon dioxide to acetate and small amounts of 2-oxobutyrate by applying electric current to acetogenic microorganisms. The subsequent research revealed an opportunity of applying in situ water electrolysis and microbes for the efficient production of other value-added commodities. Information about chemicals that can be produced in bioelectrochemical systems can be found in [9] and [10]. Hydrogen-oxidizing bacteria (HOB), the metabolic growth of which is based on the use of hydrogen as an electron donor and oxygen as an electron acceptor, were shown to be promising microorganisms for the reduction of carbon dioxide to a wide range of value-added products [11]. Volova et al. [12] found that the biological value of proteins synthesized by different strains of hydrogen-oxidizing bacteria is sufficient to consider them as a potential protein source for human and animal nutrition. Moreover, research is currently carried out into HOB-based single cell protein production. For instance, Matassa et al. [13] used autotrophic hydrogen-oxidizing bacteria to recycle ammonia recovered by air stripping from a wastewater treatment plant and captured $CO_2$, together with hydrogen and oxygen produced by water electrolysis, to food and feed [13, 14]. Furthermore, a pilot plant has been constructed in Belgium within the framework of a Power-to-Protein project, which produces single cell protein with a targeted capacity of 1 kg–2 kg per day [15]. However, these processes require external supply of hydrogen and oxygen to the bioreactors where the HOB are being cultivated. The application of bioelectrochemical system with in situ water electrolysis could provide a solution for overcoming the mass transfer limitations of this process, and could thus be considered a prospective strategy for renewable electrical energy storage. Torella et al. [16] reported development of a scalable integrated bioelectrochemical system using HOB for carbon dioxide conversion into biomass and isopropyl alcohol with maximum bioelectrochemical efficiencies of 17.8% and 3.9%, respectively. A distinctive feature of this BES was the use of a cobalt phosphate (CoPi) anode, which is capable of performing oxygen evolution reaction (OER) at low overpotentials at a neutral pH. The same anode material was used in combination with a cobalt-phosphorus (Co-P) alloy cathode in the studies of Liu et al. [17] to establish an effective water splitting system for HOB conversion into biomass at an efficiency of approximately 55% within a period of six days at an applied potential of 2.0 V. In addition to biomass, polyhydroxybutyrate (PHB), which is considered an intermediate compound in microbial assimilation of carbon dioxide, was synthesized with a 36% energy efficiency. Furthermore, different fusel alcohols were produced with efficiencies ranging from approximately 15% to 30%. Hybrid biological-inorganic (HBI) systems, which couple microorganisms with chemical catalysts to derive value-added products, have also been applied, for example, to ammonia [18] and bacterial biomass production [19].

Nevertheless, upscaling of bioelectrochemical processes for HOB cultivation requires overcoming the inherent constraints of low energy efficiency. The target of the present study is to develop a scalable energy efficient system for cultivation of hydrogen-oxidizing bacteria. The effects of various oxygen evolution (OER) catalysts are extensively reported in the literature for alkaline water electrolyzers, but there are only a few studies of electrolyzer cell performance in bioreactors with pH-neutral conditions so far. Further, a simplified mathematical model is introduced, based on models developed for traditional water electrolyzers. The model parameters are tuned and the model is verified by experimental results. The model is applied to quantitatively evaluate and compare possible overvoltage sources in the system with various electrode materials.

This paper is organized as follows. The characteristics of the in situ water electrolysis, initial HOB cultivation results with in situ water electrolysis, the experimental setup used for electrode material tests, the procedure describing in situ formation of coatings, and the simplified electrolyzer cell voltage model are introduced in Section 2. The cell voltage model parameters are fitted by experimental results, and the model is applied to describe the performance of the selected electrode materials in Section 3. Finally, Section 4 concludes the paper.

## 2. Materials & methods

This section first defines the special characteristics of the in situ water electrolysis compared with traditional water electrolyzers. HOB cultivation results with in situ water electrolysis are shown. Further, the experimental setup and methods applied for electrolyzer cell studies in this paper, including the analytical model used to describe the operation characteristics of the electrolytic cell, are introduced.

### 2.1. In situ water electrolysis characteristics

One of the key issues of the gas-fermentation-based hydrogen-oxidizing bacteria production is the mass transfer of the hydrogen gas to the cultivation medium, even though a hydrogen gas conversion efficiency up to 81% has been reported [13]. The mass transfer problems can be effectively avoided by BES, where the in situ water electrolysis takes place directly in the cultivation medium. However, the in situ water electrolysis imposes some constraints on the system. Firstly, the temperatures and pressures must be in a favorable range for the HOB. Secondly, the current densities applied to the water electrolysis must be limited to levels not harming the HOB. Finally, numerous requirements are set on the electrolyte, which also acts as a cultivation medium, and the electrodes themselves. Contrary to the traditional alkaline water electrolysis, the cultivation medium must offer an almost pH-neutral environment for the bacteria. This constraint is connected to the kinetically sluggish oxygen evolution reaction (OER), which produces a high activation overvoltage. Further, the side reactions producing toxic compounds must be prevented. In practice, these limitations lead to a significantly lower conductivity of the electrolyte compared with the traditional alkaline electrolysis. Therefore, to achieve an acceptable energy efficiency of the water electrolysis, relatively low current densities have to be applied, which leads to large electrode areas, yet the distance between the electrodes is minimized. Because of the large electrode area, low-cost electrode materials are preferred. Finally, the electrode materials must be corrosion resistant not to release any toxic compounds to the cultivation medium.

### 2.2. HOB cultivation experiments with in situ water electrolysis

The cultivation of HOB with in situ water electrolysis has been successfully tested in a small scale electrobioreactor [20]. The research utilized a BES with internal liquid volume of 60 ml as shown in Fig. 1a. $CO_2$ gas was fed to the reactor, while hydrogen and oxygen for the microbial growth and $CO_2$ fixation were generated inside the reactor vessel at a stainless steel cathode and an iridium oxide coated titanium anode. The electrodes were manufactured from wires of aforementioned materials which were looped in coils so that the surface of each electrode was 13 $cm^2$.

In Fig. 1b, the biomass increase of a hydrogen enrichment culture is presented. The culture was a mixed population of yet unidentified species, which had evolved at least some resistance towards the BES environment. The bioreactor was fed with 0.13 $g\,h^{-1}$ gaseous $CO_2$, and supplied with electrolysis current of 18 mA, which roughly equals current density of 1 $mA\,cm^{-2}$ at the surface of the electrodes, with average cell voltage of 2.31 V.

The cell mass increases in linear fashion as the growth is limited by the availability of hydrogen. Assuming faradic efficiency of unity for the electrolysis of water and complete consumption of the hydrogen, the apparent biomass yield from hydrogen was calculated to be 2.5 $g_{biomass}/mol_{H_2}$. Matassa et al. have collected biomass to hydrogen

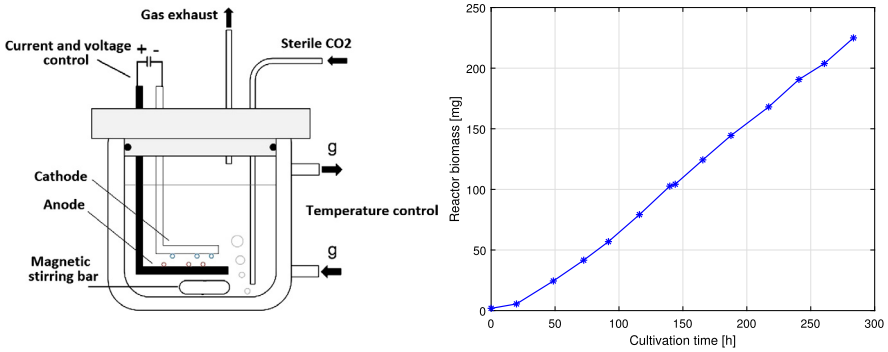


**Fig. 1.** Experimental setup used for the cultivation tests: (a) scheme of the small-scale in-situ electrolysis bioelectrochemical system, and (b) biomass increase of a mixed hydrogen enrichment culture.

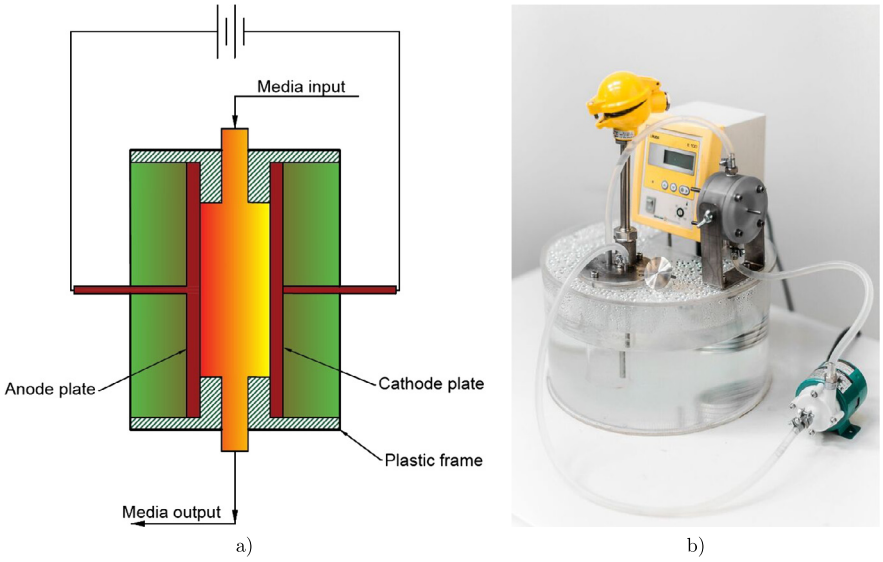


**Fig. 2.** Experimental setup used for the electrolysis tests: (a) cross section of the electrolyzer cell, (b) photo of the experimental setup.

yields for various HOB species cultivated with gaseous hydrogen feed [13].

The published values range between 1.12 $g_{biomass}/mol_{H_2}$–4.64 $g_{biomass}/mol_{H_2}$, therefore the HOB cultivation with in situ electrolysis gives biomass yield comparable to the gaseous $H_2$ feed cultivation, but without the need for handling and storage of flammable, and potentially explosive, hydrogen gas and hydrogen – oxygen gas mixtures.

The volumetric productivity of biomass during the cultivation test is below 15 $mg\,l^{-1}\,h^{-1}$ while the hydrogen production is the limiting factor for the growth. Therefore, the hydrogen production rate must be improved to enhance the volumetric productivity of the electrobioreactor. Therefore, the current density or electrode area must be increased to improve the productivity. In this article, the electrode materials are studied to enhance the current density without lowering the efficiency.

### 2.3. Experimental electrode material study setup

The experimental setup is presented in Fig. 2. The setup consists of the following elements: (i) an electrolyzer cell with a cross-sectional area of 2.6 $cm^2$ and an initial distance of 3 mm between the electrodes, (ii) a WaveNow potentiostat to conduct electrochemical measurements, (iii) a water bath with a submerged Lauda heater to keep the system optimal for the bacterial cultivation temperature of 33 °C, and (iv) a constant flow pump to circulate the medium through the external vessel equipped with the temperature measurement. Different combinations of electrode materials, such as stainless steel (SS), nickel (Ni), graphite (C), platinum (Pt), cobalt phosphate (CoPi), nickel-iron (NiFe), and iridium dioxide ($IrO_2$) deposited onto a titanium substrate, were tested. Stainless steel is widely used material because of the relatively low cost and high corrosion resistance in most environments. Applicability of SS 304 material for HOB cultivations was first studied by [16], while the effect of stainless steel or carbon surface modification by CoPi or CoP electrocatalysts was further investigated in the subsequent state of the art studies of the same research group [17, 18, 19]. However, HOB have showed to have effect on the corrosion of the low carbon steels [21]. Further, the selected 316L has been mentioned to be vulnerable to microbial corrosion, and some other steel should be selected if uncoated electrodes are used for longer periods of time [22]. Platinum is widely used as electrode material because of its stability despite the high cost. Nickel based metals are widely used in alkaline water electrolyzers, and therefore, used as a reference for the other materials [23]. Graphite is also stable, but not highly catalytic material. CoPi coatings are shown to be self healing and biocompatible in the literature [17]. $IrO_2$ coated anode is found to be a promising candidate in the HOB cultivation experiments described above. Linear sweep voltammetry (I–V) was applied to measure the cell voltage as a function of cell current. The sweep rate of the linear sweep voltammetry was selected to be 10 $mV\,s^{-1}$ to mitigate the effect of cell capacitances.

The mineral medium, used for the bioelectrochemical cultivation of hydrogen-oxidizing bacteria prepared according to the DSM-81-LO4 recipe at the VTT Technical Research Centre of Finland, was applied as an electrolyte in the study. One liter of the medium solution con-

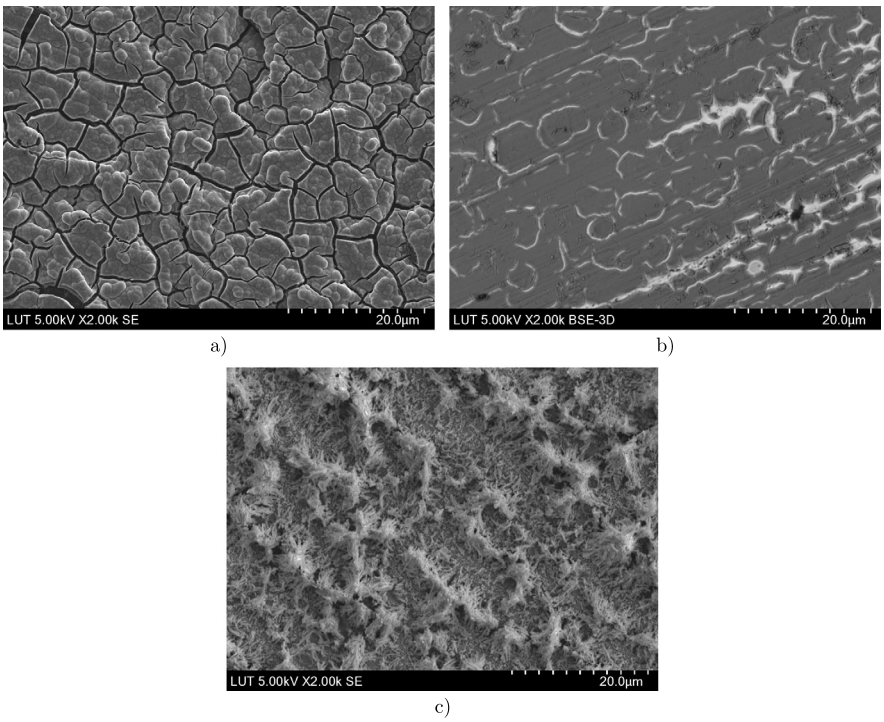


**Fig. 3.** Scanning electron microscope (SEM) images of the cobalt phosphate (CoPi) coating onto (a) graphite substrate, (b) stainless steel substrate, and (c) nickel-iron (NiFe) coating onto stainless steel substrate.

tained distilled water, 50 ml of phosphate buffer, 2.3 g ($KH_2PO_4$), 2.9 g ($Na_2HPO_4$), 2 ml ($NH_4$)(Fe)(citrate), 0.005 g of ferric ammonium citrate (16% Fe), 10 ml of ($NaHCO_3$) solution, 0.5 g ($NaHCO_3$), mineral salts, 5.45 g ($Na_2SO_4$), 1.19 g ($(NH_4)_2SO_4$), 0.5 g ($MgSO_4 \cdot 5H_2O$), 0.0117 g ($CaSO_4 \cdot 2H_2O$), 0.0044 g ($MnSO_4 \cdot 1H_2O$), 0.005 g ($NaVO_3$), and 5 ml of trace element solution. 500 ml of trace element stock solution was made from 0.05 g ($ZnSO_4 \cdot 7H_2O$), 0.15 g ($H_3BO_3$), 0.1 g ($CoCl_2 \cdot 6H_2O$), 0.005 g ($CuCl_2 \cdot 2H_2O$), 0.01 g ($NiCl_2 \cdot 6H_2O$), and 0.015 g ($Na_2MoO_4$). The phosphate buffer, the ammonium iron (III) citrate, the mineral salts, and the trace element solutions were autoclaved separately. The vitamin solution ($NaHCO_3$) was filter sterilized. The solutions were combined aseptically at room temperature. The pH and conductivity of the medium, measured before and after the electrolysis tests, were 7 and 12 mS $cm^{-1}$, respectively.

### 2.4. In situ catalyst formation

Electrodeposition of coatings based on earth-abundant first-row transition metals such as Co and Fe–Ni is considered an efficient method for the electrode surface structure modification and enhancement of the electrochemical activity. In the present study, in situ preparation of coatings was performed in the experimental setup described in the previous section based on the electrodeposition strategies adopted from [16] and [24]. Cobalt phosphate (CoPi) coating was electrodeposited onto graphite and stainless steel plates (substrates) in a solution containing 0.1 M $KH_2PO_4$ and 0.5 mM $Co(NO_3)_2 \cdot 6H_2O$ and 250 ml of distilled deionized water. Pretreatment of the electrode samples included polishing with sand paper and rinsing with acetone and deionized water. Electrolytic deposition was carried out by bulk electrolysis at 2 V for 5 h for the graphite substrate and for 3 h for the stainless steel substrate. Graphite and stainless steel were used as the auxiliary and reference electrode for the corresponding experiments in a two-electrode system. Solution with two times increased concentration of $Co_{2+}$ was also deposited onto the stainless steel substrate to investigate the influence of the increased cobalt mass on the coating structure and the electrochemical performance of the synthesized catalyst.

In situ formation of nickel-iron (NiFe) coating was carried out by the bulk electrolysis method at 2.8 V for 15 min in the solution containing 0.1 M $Na_2SO_4$, 0.25 M $NiSO_4 \cdot 6H_2O$, 0.25 M $FeSO_4 \cdot 7H_2O$, and 250 ml of distilled deionized water. A small amount of $H_2SO_4$ was added to the solution to adjust the pH to 2. A stainless steel plate with the aforementioned pretreatment was used as a substrate for the electrolytic deposition of the nickel-iron (NiFe) film. Scanning electron microscope (SEM) images of the obtained cobalt phosphate (CoPi) and nickel-iron (NiFe) structures are presented in Fig. 3.

### 2.5. Cell model

In neutral conditions (pH=7), the water electrolysis is described by the following electrochemical reactions [7]. Oxidation half-reaction at the anode–oxygen evolution reaction (OER):

$$2H_2O \longrightarrow O_2 + 4H^+ + 4e^-, E_0 = 0.817 \text{ V} \quad (1)$$

Reduction half-reaction at the cathode–hydrogen evolution reaction (HER):

$$4H_2O + 4e^- \longrightarrow 2H_2 + 4OH^-, E_0 = -0.413 \text{ V} \quad (2)$$

The overall reaction in the electrolytic cell:

$$2H_2O + \text{electrical energy} \longrightarrow O_2 + 2H_2, E_0 = -1.23 \text{ V} \quad (3)$$

The above equations demonstrate that the equilibrium or reversible cell voltage, which is the lowest potential required for the electrolysis to take place at 25 °C and 1 atm, is equal to 1.23 V. However, in practice, higher voltages are required to dissociate water; this is due to the additional overvoltages presented in the following equation:

$$U_{cell} = U_{rev} + U_{ohm} + U_{act} + U_{con}, \quad (4)$$

where $U_{cell}$ is the cell voltage, $U_{rev}$ is the reversible open circuit voltage, $U_{ohm}$ is the overvoltage caused by ohmic losses in the cell elements, $U_{act}$ is the activation overvoltage caused by electrode kinetics, and $U_{con}$ is the concentration overvoltage caused by mass transport processes [1].

In electrolysis, the production of hydrogen and oxygen is directly proportional to the mean value of the current flowing through the electrolyzer cell. Thus, the hydrogen and oxygen production rates (mol $s^{-1}$) of a single electrolytic cell can be expressed as:

$$f_{H_2} = \eta_F \frac{i_{cell} A_{cell}}{zF}, \tag{5}$$

where $z$ ($z = 2$ and 4 for hydrogen and oxygen, respectively) is the number of moles of electrons transferred in the reaction, $F$ is the Faraday constant ($9.6485\times10^4$ C $mol^{-1}$), $i_{cell}$ is the current density (A $cm^{-2}$), $A_{cell}$ is the effective cell area ($cm^2$), and $\eta_F$ is the Faraday efficiency, also known as the current efficiency. In this study, the Faraday efficiency can be assumed to be unity because there should be no leakage currents, and further, as the product gas is a mixture of hydrogen and oxygen, there is no leakage of hydrogen to the oxygen line as in traditional electrolyzers [25]. Therefore, the hydrogen production rate can be directly estimated based on current, and the voltage eventually describes the energy efficiency of the cell.

A simplified model to describe the electrolytic cell voltage behavior as a function of current is introduced. The open-circuit voltage can be described using the Nernst equation [26]

$$U_{rev} = U^0_{rev} + \frac{RT_{el}}{zF} \ln\left(\frac{p_{H_2} \cdot p_{O_2}^{1/2}}{p_{H_2O}}\right), \tag{6}$$

where $U^0_{rev}$ is the reversible cell voltage, $R$ is the universal gas constant (8.3144621 J $mol^{-1}$ $K^{-1}$), and $T_{el}$ is the temperature. Further, $p_{H_2}$, $p_{O_2}$, and $p_{H_2O}$ are the hydrogen, oxygen, and water partial pressures.

The reversible cell voltage is defined as a function of temperature; for example, for a PEM electrolyzer cell in [27] and for an alkaline electrolyzer cell with the KOH electrolyte in [28]. However, in this simplified case, the open-circuit cell voltage under constant operating temperature and atmospheric pressure is considered as one parameter to be found by the curve fitting of the measured data.

The ohmic overpotential is mainly caused by the voltage across the cultivation medium with the conductivity in the range of 10 mS $cm^{-1}$ as the conductivity of titanium or stainless steel electrodes is roughly 2.5 kS $cm^{-1}$. Therefore, the ohmic overpotential can be expressed as

$$U_{ohm} = \frac{\delta_m i_{cell}}{\sigma_m}, \tag{7}$$

where $\delta_m$ is the distance between the electrodes in (cm), and $\sigma_m$ is the conductivity of the medium in (S $cm^{-1}$).

The activation overpotential is typically described by using the Butler–Volmer equation [29]

$$U_{act} = \frac{RT_{el}}{\alpha_{an} F} \operatorname{arcsinh}\left(\frac{i_{cell}}{2i_{o,an}}\right) + \frac{RT_{el}}{\alpha_{cat} F} \operatorname{arcsinh}\left(\frac{i_{cell}}{2i_{o,cat}}\right), \tag{8}$$

where $\alpha$ is the charge transfer coefficient for the anode and the cathode separately, and $i_o$ is the exchange current density on the electrode surfaces. The charge transfer coefficients and the exchange current densities are experimentally defined as a function of temperature for example in [30].

Finally, the simplified model for the cell voltage as a function of current can be expressed as

$$U_{cell} = U_{rev} + \frac{\delta_m i_{cell}}{\sigma_m} + \alpha \operatorname{arcsinh}\left(\frac{i_{cell}}{2i_0}\right), \tag{9}$$

where $U_{rev}$, $\sigma_m$, $\alpha$, and $i_0$ are the parameters to be fitted by the experimental data.

## 3. Results & discussion

Graphite was used as an electrode material for the first bioelectrochemical cultivation tests of an acetogenic microorganism in [8]. Nickel and stainless steel have traditionally been used with alkaline electrolyzers whereas noble metals and their oxides, such as platinum and iridium dioxide, are known for their high catalytic activity. Therefore, the performance of the aforementioned materials was studied for the electrolyte introduced in Section 2. The potential of coated electrodes prepared by electrodeposition of Co and a Fe–Ni alloy as a possible substitute for electrodes made of precious metals was also evaluated.

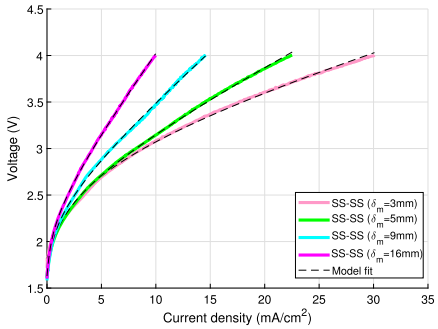


**Fig. 4.** Experimental results of water electrolysis with stainless steel (SS) electrodes, obtained with a variable distance, and the modeling results with Eq. (9).

Both hydrogen and oxygen are important in the cultivation of HOB, and thus, a membrane-free electrolyzer cell prototype was used for the electrolysis tests. The absence of a membrane makes it possible to decrease the distance between the electrodes and increase the electrical efficiency, which is especially important in pH-neutral conditions. However, the flow of biomass through the electrolyzer can become an issue at very low distances between the electrodes. Hence, the electrode materials were tested at distances varying from 3 mm to 16 mm to collect the voltage-current characteristics of the electrolyzer cell as a function of distance between the electrodes. In the present section, the linear sweep voltammetry results for various anode and cathode material sets of the in situ water electrolysis are presented and analyzed with the developed cell model.

### 3.1. Stainless steel electrodes

First, stainless steel electrodes were used as the anode and the cathode. The main solutes of the Sanmac 316L alloy per weight are: chromium 17.0%, nickel 10.1%, molybdenum 2.0%, and manganese 1.6%. The distance of the electrodes was varied to study the effect of distance on the cell voltage. Further, the results are used to verify the simplified cell model. As only the distance between the electrodes is changed and resistive conduction losses are described by the medium conductivity, all the model parameters should match each other in all cases. A minimum distance of 3 mm between the electrodes was selected to limit the flow resistance of the electrolyte. Further, it was assumed that distances exceeding 10 mm cannot be used because of the low conductivity of the electrolyte. The cell voltage as a function of current density is shown in Fig. 4.

The distance between the electrodes has a significant impact on voltage owing to the high ohmic losses caused by the low conductivity of the medium. If the voltage efficiency of the electrolysis is required to be higher than 50%, considering the thermoneutral voltage of 1.48 V, the current density cannot exceed the value of 10 mA $cm^{-2}$ at the distance of 3 mm between the electrodes as the current densities in commercial alkaline electrolyzers are up to 500 mA $cm^{-2}$ [31]. At greater distances the allowed current density would be even lower. Therefore, it can be concluded that the distance between the electrodes should be as short as possible to achieve a high efficiency and a compact structure. The parameters $U_{rev}$, $\sigma_m$, $\alpha$, and $i_0$ in Eq. (9) were determined using experimental voltage and current data and the method of nonlinear least square regression, and presented in Table 1. Further, the reversible voltage, the ohmic voltage, and the activation voltage terms are presented separately in Fig. 5.

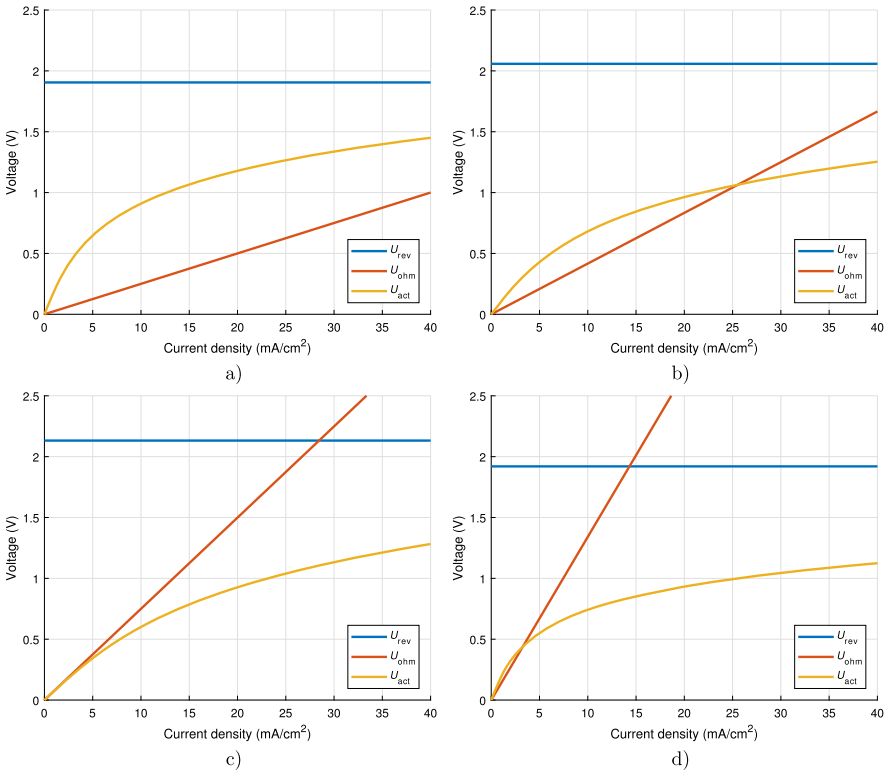


**Fig. 5.** Reversible voltage, ohmic overvoltage, and activation overvoltage as a function of current density for the water electrolysis experiments with a variable distance between the stainless steel electrodes: (a) $\delta_m = 3$ mm, (b) $\delta_m = 5$ mm, (c) $\delta_m = 9$ mm, and (d) $\delta_m = 16$ mm.

**Table 1**
Experimentally fitted parameters of the simplified cell model with stainless steel electrodes.

| $\delta_m$ (mm) | $U_{rev}$ (V) | $\sigma_m$ (S cm$^{-1}$) | $\alpha$ (-) | $i_0$ (A cm$^{-1}$) |
|---|---|---|---|---|
| 3 | 1.905 | 0.012 | 0.393 | 0.0010 |
| 6 | 2.058 | 0.012 | 0.425 | 0.0021 |
| 9 | 2.132 | 0.012 | 0.530 | 0.0036 |
| 16 | 1.92 | 0.012 | 0.278 | 0.0007 |

We can see that the ohmic overpotential becomes higher than the activation overpotential at relatively moderate current densities of 3 mA cm$^{-1}$–25 mA cm$^{-1}$ depending on the distance between the electrodes. At great distances between the electrodes the ohmic overpotential even exceeds the reversible voltage. The reversible voltage and the activation overpotential are almost the same with all distances between the plates, as supposed, that supports the use of the simplified model.

### 3.2. Anode material comparison

According to Eq. (1), the potential of the anode half reaction is higher than the potential of the cathode half reaction. Therefore, all the studied materials were applied to the anode as the cathode is made of stainless steel. The cell voltages with different anode materials with the electrode distance of 3 mm are presented as a function of current density in Fig. 6.

As can be seen in Fig. 6, the anode material has a significant effect on the cell voltage, especially at higher current densities. Graphite clearly exhibits the worst performance with the highest cell voltage, and the nickel and platinum anodes have voltages relatively close to each other. The iridium-dioxide-coated anode is obviously the most favorable anode material of the studied materials. With the iridium dioxide, a current density of 15 mA cm$^{-2}$ can be achieved with a voltage efficiency of 50%. The reversible voltage, the ohmic voltage, and the activation voltage terms as a function of current density with different anode materials are compared with each other in Fig. 7 and the model parameters are shown in Table 2.

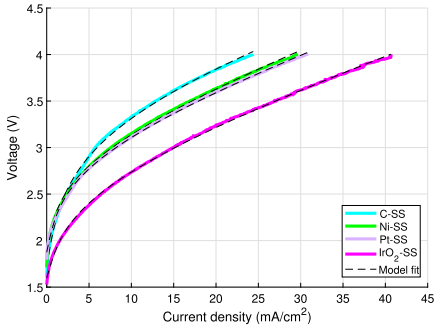


**Fig. 6.** Cell voltage as a function of current density with various anode materials and a stainless steel cathode. The solid lines indicate the measured data and the dashed lines represent the simplified model.

**Table 2**
Experimentally fitted parameters of the simplified cell model with various anode materials.

| Anode | $U_{rev}$ (V) | $\sigma_m$ (S cm$^{-1}$) | $\alpha$ (-) | $i_0$ (A cm$^{-1}$) |
|---|---|---|---|---|
| C | 2 | 0.012 | 0.455 | 0.0010 |
| Ni | 2 | 0.012 | 0.338 | 0.0007 |
| Pt | 1.975 | 0.012 | 0.332 | 0.0007 |
| $IrO_2$ | 1.766 | 0.012 | 0.351 | 0.0013 |

The material selection significantly affects the reversible voltage and the activation voltage. The iridium oxide yields a slightly lower reversible voltage compared with the other materials. The activation overpotential is highest in the case of the graphite anode as the activation overpotentials with the other materials are in the same range with each other. Furthermore, the resistive voltage loss is mainly caused by

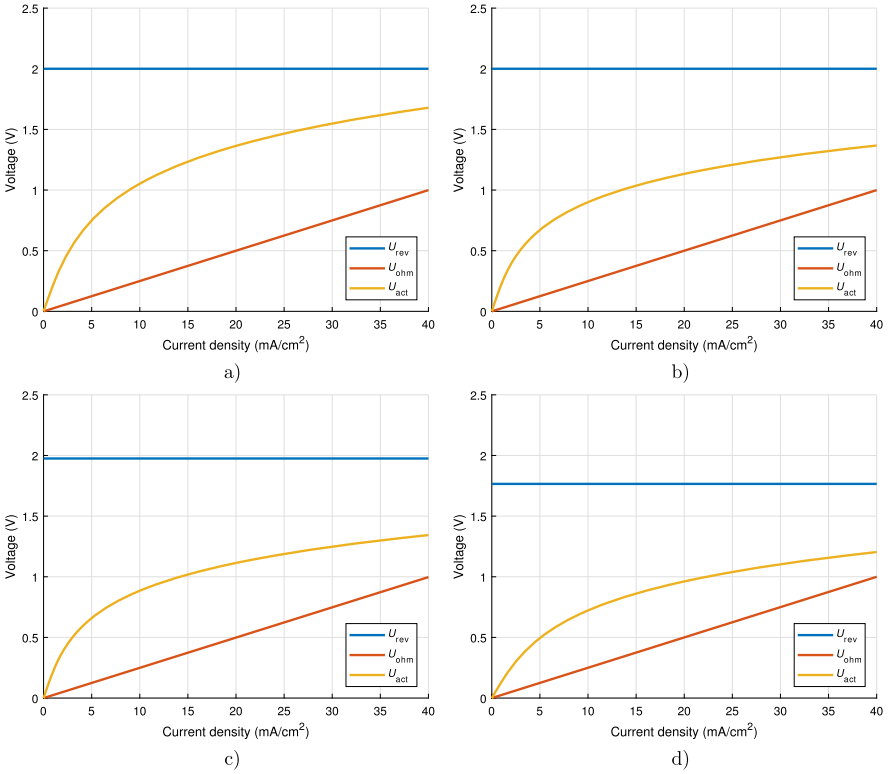


**Fig. 7.** Separated overvoltages for the water electrolysis experiments with different anode materials: (a) graphite (C), (b) nickel (Ni), (c) platinum (Pt), and (d) iridium dioxide ($IrO_2$).

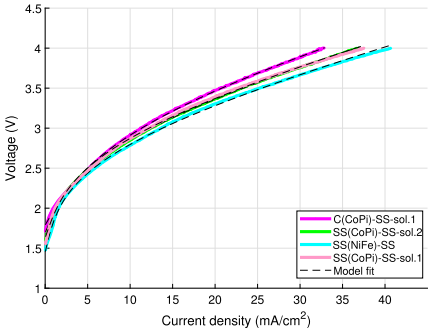


**Fig. 8.** Cell voltage as a function of current density with coated electrodes used as the anodes and stainless steel as the cathode.

the low-conductivity electrolyte medium, and thus, the electrode material has practically no impact on it.

### 3.3. Coated electrodes

Subsequently, coated electrodes were applied to the anode and stainless steel was used as the cathode. The cell voltages with different coated anode materials with the electrode distance of 3 mm are presented as a function of current density in Fig. 8.

It can be clearly seen from Fig. 8 that coated electrodes can be considered an attractive alternative for catalysts made of precious metals. Electrodeposition of Co and the Ni-Fe alloy enables substrate surface structure modification by enhancement of the electrochemically active surface area, which is well shown in Fig. 3. The obtained highly ordered CoPi coatings exhibited a better performance than the Pt anode, whereas the performance of the Ni-Fe film was comparable with the $IrO_2$ anode. A current density of approximately 14 mA cm$^{-2}$ was achieved with a voltage efficiency of 50% when using stainless steel coated with the Ni-Fe alloy. It was also found that the substrate material had an effect on the electrochemical performance of the electrode. The performance of the CoPi coating on the graphite substrate was slightly lower than the performance of the same coating electrodeposited onto stainless steel substrates. The performances of the CoPi coatings electrodeposited onto the stainless steel substrate from solution 1 and solution 2 with 0.5 and 1 mM concentrations of $Co_{2+}$, respectively, were similar.

**Table 3**
Experimentally fitted parameters of the simplified cell model with various coated electrodes used as the anode materials.

| Anode | $U_{rev}$ (V) | $\sigma_m$ (S cm$^{-1}$) | $\alpha$ (-) | $i_0$ (A cm$^{-1}$) |
|---|---|---|---|---|
| C(CoPi-sol.1) | 1.790 | 0.012 | 0.443 | 0.0014 |
| SS(CoPi-sol.1) | 1.630 | 0.012 | 0.359 | 0.0006 |
| SS(CoPi-sol.2) | 1.695 | 0.012 | 0.370 | 0.0009 |
| SS(NiFe) | 1.449 | 0.012 | 0.338 | 0.0004 |

The reversible voltage, the ohmic voltage, and the activation voltage terms as a function of current density with different coated anodes are compared with each other in Fig. 9 and the model parameters are shown in Table 3.

### 3.4. Cathode material comparison

Finally, the most promising anode materials were also used as the cathode material to see if the performance can be further improved. The cell voltages with different anode and cathode material combinations are presented as a function of current density in Fig. 10, and the model parameters are summarized in Table 4.

Current densities of 25, 15, and 10 mA cm$^{-2}$ were achieved with the voltage efficiency of 50% for $IrO_2$, Pt, and SS used for both the anode and the cathode. In the previous research [16], HOB managed to tolerate and grow at current densities up to approximately 4 mA cm$^{-2}$ with 2.5 V cell potential. Further increase of the driving voltage up to 3 V resulted in the exponential increase of the cell densities and the

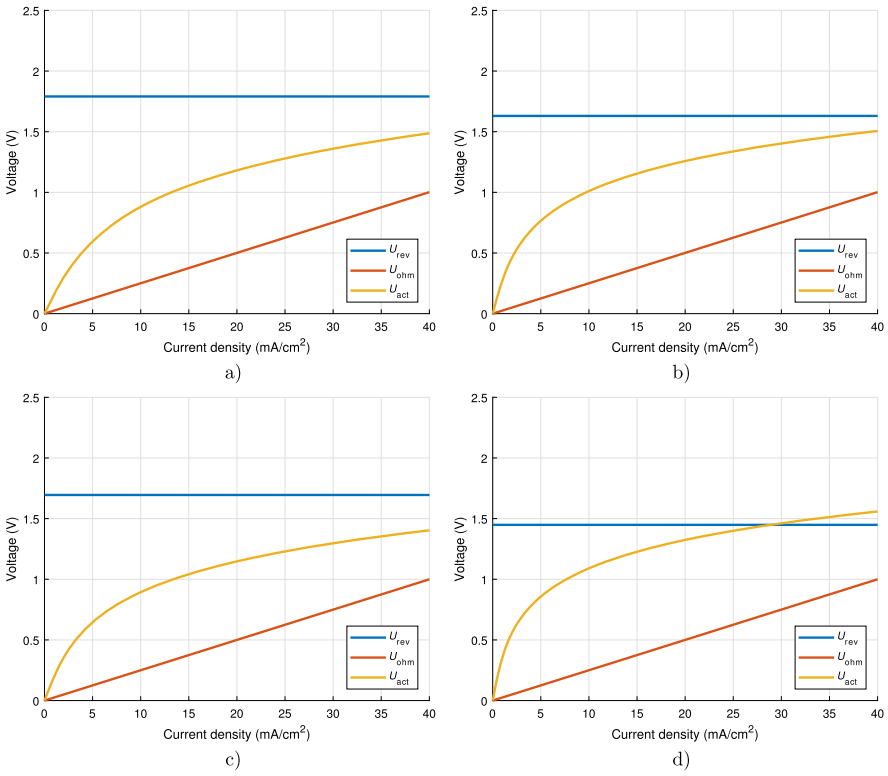


**Fig. 9.** Separated overvoltages for the water electrolysis experiments with different coated electrodes used as the anode materials: (a) graphite coated with CoPi using solution 1, (b) stainless steel coated with CoPi using solution 1, (c) stainless steel coated with CoPi using solution 2, and (d) stainless steel coated with NiFe.

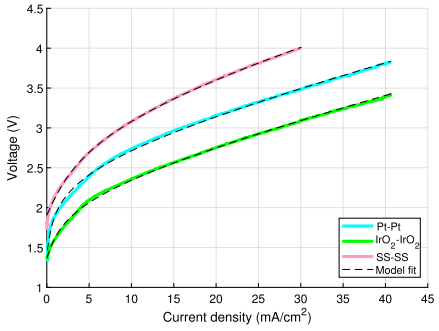


**Fig. 10.** Cell voltage as a function of current density with the best-performing anode and cathode materials.

**Table 4**
Experimentally fitted parameters of the simplified cell model with the best-performing electrode materials.

| An./Cath. | $U_{rev}$ (V) | $\sigma_m$ (S cm$^{-1}$) | $\alpha$ (-) | $i_0$ (A cm$^{-1}$) |
|---|---|---|---|---|
| Pt-Pt | 1.4 | 0.012 | 0.255 | 0.0002 |
| $IrO_2$-$IrO_2$ | 1.366 | 0.012 | 0.227 | 0.0004 |

highest reported value for the current density, which bacteria managed to tolerate, was 11 mA cm$^{-2}$.

It is important to note, that there was no substantial increase in the performance when using CoPi and Ni-Fe coated catalysts for both electrodes in comparison with the experiments where SS was used as the cathode material. Thus, we can state that the aforementioned coatings are catalytically active for oxygen evolution reaction (OER) but do not exhibit high catalytic activity for hydrogen evolution reaction (HER). Even though $IrO_2$ shows the best performance as the anode and cathode material, the SS performance is still acceptable when considering the high manufacturing cost of catalysts made of precious metals. Furthermore, the SS can be considered a potential cost-effective substrate material for electrodeposition of coatings. It can be concluded that in a neutral environment the cathode material also has a significant effect on the water electrolysis performance. The cell overpotentials with different electrode material combinations are shown in Fig. 11.

The reversible voltage with both the platinum- and iridium-dioxide-coated cathodes is significantly lower than with the stainless steel cathode. Further, the iridium-dioxide-coated cathode exhibits a lower activation overpotential than platinum.

## 4. Conclusions

In the present paper, a simplified cell model was proposed to describe the cell voltage components as a function of current density. It is noteworthy that the chemical formulation of the electrolyte significantly affects the electrical resistance of the electrolysis cell and thereby the energy efficiency of the whole process. The developed model was implemented to analyze the applicability of numerous electrode materials for the in situ electrolysis of a pH-neutral medium for bioelectrochemical cultivation of hydrogen oxidizing bacteria. The model enables quantitive evaluation of the reversible voltage, ohmic overpotential, and activation overpotential for different sets of electrode materials.

The obtained highly ordered CoPi and Ni-Fe coatings exhibited an oxygen evolution reaction (OER) performance exceeding that of the Pt anode and being comparable with the $IrO_2$ anode. However, the aforementioned coatings did not show a substantial improvement in performance for the hydrogen evolution reaction (HER) compared with the stainless steel cathode. Based on this observation, we can conclude that additional research is required to find suitable coatings with high electrocatalytic performance for the HER.

The lowest cell voltage as a function of current density was reached with the $IrO_2$ coating both at the anode and the cathode. With the stainless steel electrodes, the same voltage level was achieved at roughly 50% lower current densities compared with the $IrO_2$-coated electrodes.

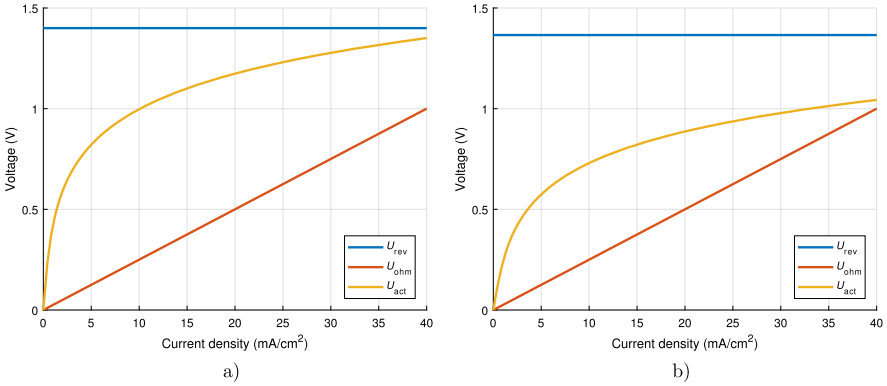


**Fig. 11.** Separated overvoltages for the water electrolysis experiments of the best electrode material combinations: (a) platinum-platinum (Pt–Pt), and (b) iridium-iridium ($IrO_2$–$IrO_2$).

Despite this, the stainless steel can be considered a potential cost-effective substrate material for preparation of coatings in electrobioreactors with in situ electrolysis of media.

A detailed energy efficiency analysis of the bioelectrochemical system and an analysis of the effects of the in situ water electrolysis on the microbial growth, e.g. maximum allowable current density, will be conducted in the further research into the topic.

## Declarations

### *Author contribution statement*

Georgy Givirovskiy, Vesa Ruuskanen, Jero Ahola, Leo Ojala, Michael Lienemann, Petteri Kokkonen: Conceived and designed the experiments; Performed the experiments; Analyzed and interpreted the data; Contributed reagents, materials, analysis tools or data; Wrote the paper.

### *Funding statement*

This work was supported by Finnish Academy of Science for "MOPED – Microbial Oil and Proteins from Air by Electricity-Driven Microbes" project funding under number 295866.

### *Competing interest statement*

The authors declare no conflict of interest.

### *Additional information*

No additional information is available for this paper.

## References

[1] A. Ursúa, L. Gandía, P. Sanchis, Hydrogen production from water electrolysis: current status and future trends, Proc. IEEE 100 (2) (2012) 410–426.
[2] I. Dincer, C. Acar, Review and evaluation of hydrogen production methods for better sustainability, Int. J. Hydrog. Energy 40 (34) (2014) 11094–11111.
[3] T. Kousksou, P. Bruel, A. Jamil, T. El Rhafiki, Y. Zeraouli, Energy storage: applications and challenges, Sol. Energy Mater. Sol. Cells 120 (PART A) (2014) 59–80.
[4] United Nations Environment Programme, The hydrogen economy: a non-technical review, https://www.unenvironment.org/resources/report/hydrogen-economy-non-technical-review, 2006.
[5] S.E. Hosseini, M.A. Wahid, Hydrogen production from renewable and sustainable energy resources: promising green energy carrier for clean development, Renew. Sustain. Energy Rev. 57 (2016) 850–866.
[6] M. Lehner, R. Tichler, H. Steinmüller, M. Koppe, Power-to-Gas: Technology and Business Models, Springer International Publishing, New York, 2014.
[7] Y. Cheng, S.P. Jiang, Advances in electrocatalysts for oxygen evolution reaction of water electrolysis-from metal oxides to carbon nanotubes, Prog. Nat. Sci. 25 (6) (2015) 545–553.
[8] K.P. Nevin, T.L. Woodard, A.E. Franks, Z.M. Summers, D.R. Lovley, Microbial electrosynthesis: feeding microbes electricity to convert carbon dioxide and water to multicarbon extracellular organic compounds, mBio 1 (2) (2010), http://mbio.asm.org/content/1/2/e00103-10.full.pdf.
[9] S. Bajracharya, M. Sharma, G. Mohanakrishna, X. Dominguez Benneton, D.P. Strik, P.M. Sarma, D. Pant, An overview on emerging bioelectrochemical systems (BESs): technology for sustainable electricity, waste remediation, resource recovery, chemical production and beyond, Renew. Energy 98 (2016) 153–170.
[10] G. Kumar, R.G. Saratale, A. Kadier, P. Sivagurunathan, G. Zhen, S.H. Kim, G.D. Saratale, A review on bio-electrochemical systems (BESs) for the syngas and value added biochemicals production, Chemosphere 177 (2017) 84–92.
[11] J. Yu, A. Dow, S. Pingali, The energy efficiency of carbon dioxide fixation by a hydrogen-oxidizing bacterium, Int. J. Hydrog. Energy 38 (21) (2013) 8683–8690.
[12] T.G. Volova, V.A. Barashkov, Characteristics of proteins synthesized by hydrogen-oxidizing microorganisms, Appl. Biochem. Microbiol. 46 (6) (2010) 574–579.
[13] S. Matassa, W. Verstraete, I. Pikaar, N. Boon, Autotrophic nitrogen assimilation and carbon capture for microbial protein production by a novel enrichment of hydrogen-oxidizing bacteria, Water Res. 101 (2016) 137–146.
[14] S. Matassa, N. Boon, I. Pikaar, W. Verstraete, Microbial protein: future sustainable food supply route with low environmental footprint, Microb. Biotechnol. 9 (5) (2016) 568–575.
[15] F. Oesterholt, S. Matassa, L. Palmen, K. Roest, W. Verstraete, Pilot scale production of single cell proteins using the power-to-protein concept future global challenges, in: 2nd International Resource Recovery Conference, 2018, pp. 1–16.
[16] J.P. Torella, C.J. Gagliardi, J.S. Chen, D.K. Bediako, B. Colón, J.C. Way, P.A. Silver, D.G. Nocera, Efficient solar-to-fuels production from a hybrid microbial–water-splitting catalyst system, Proc. Natl. Acad. Sci. 112 (8) (2015) 2337–2342.
[17] C. Liu, M. Ziesack, P.A. Silver, Water splitting – biosynthetic system with $CO_2$ reduction efficiencies exceeding photosynthesis, Science 352 (6290) (2016) 1210–1213.
[18] C. Liu, K.K. Sakimoto, B.C. Colón, P.A. Silver, D.G. Nocera, Ambient nitrogen reduction cycle using a hybrid inorganic–biological system, Proc. Natl. Acad. Sci. 114 (25) (2017) 6450–6455.
[19] C. Liu, B.E. Colón, P.A. Silver, D.G. Nocera, Solar-powered $CO_2$ reduction by a hybrid biological | inorganic system, J. Photochem. Photobiol. A, Chem. 358 (2018) 411–415.
[20] M. Wuokko, Chemolithoautotrophic Growth of Knallgas Bacteria in an Electrobioreactor Using in situ Water Electrolysis, Master's thesis, 2017, http://urn.fi/URN:NBN:fi:aalto-201705114594.
[21] R. Moreira, M.K. Schütz, M. Libert, B. Tribollet, V. Vivier, Fluence of hydrogen-oxidizing bacteria on the corrosion of low carbon steel: local electrochemical investigations, Bioelectrochemistry 97 (2014) 69–75.
[22] Sandvik, Microbiologically influenced corrosion (MIC), https://www.materials.sandvik/fi-fi/tietopankki/korroosiotietoja/wet-corrosion/microbiologically-influenced-corrosion-mic/, 2019. (Accessed 4 April 2019).
[23] M. Schalenbach, A.R. Zeradjanin, O. Kasian, S. Cherevko, A perspective on low-temperature water electrolysis – challenges in alkaline and acidic technology, Int. J. Electrochem. Sci. 13 (2018) 1173–1226.
[24] K.H. Kim, J.Y. Zheng, W. Shin, Y.S. Kang, Preparation of dendritic NiFe films by electrodeposition for oxygen evolution, RSC Adv. 2 (2012) 4759–4767.
[25] M. Schalenbach, M. Carmo, D. Fritz, J. Mergel, D. Stolten, Pressurized PEM water electrolysis: efficiency and gas crossover, Int. J. Hydrog. Energy 38 (35) (2013) 14921–14933.
[26] A. Awasthi, K. Scott, S. Basu, Dynamic modeling and simulation of a proton exchange membrane electrolyzer for hydrogen production, Int. J. Hydrog. Energy 36 (22) (2011) 14779–14786.
[27] K. Harrison, E. Hernández-Pacheco, M. Mann, H. Salehfar, Semiempirical model for determining PEM electrolyzer stack characteristics, J. Fuel Cell Sci. Technol. 3 (2) (2005) 220–223.
[28] R. LeRoy, C. Bowen, D. LeRoy, The thermodynamics of aqueous water electrolysis, J. Electrochem. Soc. 127 (9) (1980) 1954–1962.

[29] J. Larminie, A. Dicks, Fuel Cell Systems Explained, John Wiley & Sons Ltd., England, 2003.

[30] C. Biaku, N. Dale, M. Mann, H. Salehfar, A. Peters, T. Han, A semiempirical study of the temperature dependence of the anode charge transfer coefficient of a 6 kW PEM electrolyzer, Int. J. Hydrog. Energy 33 (16) (2008) 4247–4254.

[31] B. Decourt, B. Lajoie, R. Debarre, O. Soupa, The Hydrogen-Based Energy Conversion FactBook, The SBC Energy Institute, 2014.